

**NASA TECHNICAL NOTE**



**NASA TN D-7400**

**NASA TN D-7400**

**CASE FILE  
COPY**

**PERFORMANCE ANALYSIS  
OF THE ASCENT PROPULSION SYSTEM  
OF THE APOLLO SPACECRAFT**

*by John C. Hooper III*

*Lyndon B. Johnson Space Center  
Houston, Texas 77058*

1. Report No. <b>TN D-7400</b>		2. Government Accession No.		3. Recipient's Catalog No.	
4. Title and Subtitle <b>PERFORMANCE ANALYSIS OF THE ASCENT PROPULSION SYSTEM OF THE APOLLO SPACECRAFT</b>				5. Report Date <b>December 1973</b>	
				6. Performing Organization Code	
7. Author(s) <b>John C. Hooper III, JSC</b>				8. Performing Organization Report No. <b>JSC S-354</b>	
9. Performing Organization Name and Address <b>Lyndon B. Johnson Space Center Houston, Texas 77058</b>				10. Work Unit No. <b>914-50-60-07-72</b>	
				11. Contract or Grant No.	
12. Sponsoring Agency Name and Address <b>National Aeronautics and Space Administration Washington, D. C. 20546</b>				13. Type of Report and Period Covered <b>Technical Note</b>	
				14. Sponsoring Agency Code	
15. Supplementary Notes					
16. Abstract <p>This report discusses activities involved in the performance analysis of the Apollo lunar module ascent propulsion system. A description of the ascent propulsion system, including hardware, instrumentation, and system characteristics, is included. The methods used to predict the inflight performance and to establish performance uncertainties of the ascent propulsion system are discussed. The techniques of processing the telemetered flight data and performing post-flight performance reconstruction to determine actual inflight performance are discussed. Problems that have been encountered and results from the analysis of the ascent propulsion system performance during the Apollo 9, 10, and 11 missions are presented.</p>					
17. Key Words (Suggested by Author(s)) <b>Ascent Propulsion Systems      Apollo Project Propulsion System Performance      Lunar Module Postflight Analysis      Command and Performance Prediction      Service Liquid-Propellant Rocket Engines      Module</b>				18. Distribution Statement	
19. Security Classif. (of this report) <b>None</b>		20. Security Classif. (of this page) <b>None</b>		21. No. of Pages <b>42</b>	22. Price <b>Domestic, \$3.00 Foreign, \$5.50</b>

# CONTENTS

Section	Page
SUMMARY . . . . .	1
INTRODUCTION . . . . .	2
DESCRIPTION OF THE ASCENT PROPULSION SYSTEM . . . . .	3
Hardware Description . . . . .	3
Instrumentation Description . . . . .	6
PREFLIGHT ANALYSIS ACTIVITIES . . . . .	9
Program and Model Description . . . . .	9
Data Acquisition and Treatment . . . . .	11
Preflight Performance Analysis . . . . .	13
Malfunction Simulations and Special Data Requests . . . . .	16
POSTFLIGHT ANALYSIS ACTIVITIES . . . . .	17
Program and Model Description . . . . .	18
Data Acquisition and Treatment . . . . .	21
Postflight Performance Analysis . . . . .	22
DISCUSSION OF RESULTS . . . . .	24
LM-3 Results . . . . .	24
LM-4 Results . . . . .	30
LM-5 Results . . . . .	31
General Comments . . . . .	34
CONCLUDING REMARKS . . . . .	35
REFERENCES . . . . .	36
APPENDIX - Acronyms and Abbreviations . . . . .	37

## TABLES

Table		Page
I	ASCENT-ENGINE DESIGN CHARACTERISTICS AND NOMINAL PERFORMANCE . . . . .	5
II	ASCENT PROPULSION SYSTEM OPERATIONAL INSTRUMENTATION . . . . .	7
III	TYPICAL VALUES USED IN THE CALCULATION OF APS PERFORMANCE DISPERSIONS . . . . .	15
IV	EFFECT OF VARIOUS MALFUNCTIONS ON APS PERFORMANCE VALUES . . . . .	17
V	RESULTS OF LM-3 FLIGHT ANALYSIS . . . . .	25
VI	RESULTS OF LM-4 FLIGHT ANALYSIS . . . . .	30
VII	RESULTS OF LM-5 FLIGHT ANALYSIS . . . . .	33

## FIGURES

Figure		Page
1	Schematic of the APS . . . . .	4
2	Real-time telemetry (PCM) of the APS . . . . .	6
3	Telemetry (PCM and DFI) of the APS . . . . .	8
4	Preflight mission-simulation input/output . . . . .	9
5	Effect of propellant temperature on APS mixture ratio . . . . .	16
6	Effect of propellant temperature on APS engine thrust and specific impulse . . . . .	16
7	Postflight data-flow logic diagram . . . . .	22
8	LM-3 APS performance analysis results: comparison of predicted and reconstructed throat area . . . . .	26
9	LM-3 APS performance analysis results: comparison of predicted and reconstructed performance . . . . .	27

Figure		Page
10	LM-3 APS postflight performance analysis: comparison of pressure trends (flight, reconstructed, and repredicted) . . . . .	27
11	LM-3 APS flight results: predicted and actual helium source temperature . . . . .	28
12	LM-3 APS flight results: predicted and actual helium source pressure . . . . .	28
13	LM-3 APS flight results: predicted and actual helium-regulator outlet pressure . . . . .	28
14	LM-3 APS flight results: oxidizer interface pressure . . . . .	28
15	LM-3 APS flight results: fuel interface pressure . . . . .	28
16	LM-3 APS postflight performance analysis: oxidizer-feed-system differential pressure (tank bottom to engine interface) . . . . .	28
17	LM-3 APS postflight performance analysis: fuel-feed-system differential pressure (tank bottom to engine interface) . . . . .	29
18	LM-3 APS postflight performance analysis: engine chamber pressure . . . . .	29
19	LM-3 APS postflight performance analysis: ascent-stage thrust acceleration . . . . .	29
20	LM-4 APS performance analysis results: comparison of predicted and flight-reconstructed performance . . . . .	31
21	LM-5 APS postflight performance analysis: time-averaged RCS thrust . . . . .	33
22	LM-5 APS performance analysis results: comparison of predicted and reconstructed performance . . . . .	34

# PERFORMANCE ANALYSIS OF THE ASCENT PROPULSION SYSTEM OF THE APOLLO SPACECRAFT

By John C. Hooper III  
Lyndon B. Johnson Space Center

## SUMMARY

Because of the limited number of lunar module flights in the Apollo Program and the cost of the hardware involved, an understanding of the capability of the ascent propulsion system is necessary so that maximum benefit can be extracted from each flight without compromising mission safety. The accomplishment of this goal requires a method of predicting the performance of the ascent propulsion system with a high degree of accuracy and confidence.

The design function of the ascent propulsion system is to provide the velocity change necessary to take the ascent stage from the lunar surface into lunar orbit. The ascent propulsion system consists of a pressure-fed, liquid-bipropellant, ablatively cooled rocket engine and its associated propellant feed, storage, and pressurization systems.

Predicted performance for a given flight vehicle is determined by the use of a propulsion system mathematical model, which is adjusted to the particular vehicle by factors derived from component-level preinstallation and acceptance test data. A computer program, which incorporates this model, is used to simulate the operation of the propulsion system over the desired mission duty cycle. Ground test data, instrumentation accuracies, and uncertainties in the model of the propulsion system are examined to determine the uncertainty band associated with a preflight performance prediction. Also, the mathematical model is used to study the operation of the ascent propulsion system under conditions of component malfunction or other off-nominal operation.

A postflight analysis of the inflight vehicle performance is required to verify the adequacy of the preflight prediction techniques. The postflight analysis is performed with the aid of a computer program specifically developed for this task. This program uses a minimum-variance estimation technique to allow the calculation of the best statistical estimate of propulsion system performance from the available data. The overall goal of the efforts is a continuing refinement in prediction techniques, leading to increased confidence in the capabilities of the propulsion system.

The performance analysis obtained can predict the performance of the ascent propulsion system, establish realistic uncertainty bands associated with the prediction and predict the effect of selected off-nominal conditions.

## INTRODUCTION

Because of the unique requirements of the Apollo Program, the prediction, before flight, of the performance expected from the propulsion system of each spacecraft and the evaluation of inflight performance has been carried to a degree of refinement beyond that previously attempted. The refinements were necessitated by the weight criticality of the Apollo spacecraft, by the limited number of Apollo flights and the expense of the hardware involved, and by the unavailability of integrated system test data for the flight propulsion system. Weight criticality, limited number of flights, and hardware expense place a great importance on extracting maximum benefits from each flight without compromising mission safety.

A basic decision was made early in the Apollo Program to the effect that each flight propulsion system would not be tested as an integrated system. Although a ground test of the system would have reduced the reliance on analytical methods to some extent, uncertainties would still have existed because of factors such as the changing performance of the ablative engine as a function of time and the run-to-run uncertainties inherent in the system. Analytical models of some type would still be required to evaluate effects such as component replacement. Another factor involved in this decision was the incompatibility of many of the propulsion system components with the propellants selected (nitrogen tetroxide and Aerozine-50). These considerations led to the selected mode of operation in which the propulsion system, with the exception of the engine (which is subjected to a decontamination process), is not exposed to propellants until the loading operations before launch.

Given the mode of operation selected for Apollo flights, predicted performance for a given flight vehicle is determined by the use of a mathematical model of the propulsion system. The performance of the system as a function of the various operating conditions is given by characterizations of the various components of the system derived from analyses of numerous ground tests. Predicted performance for a given flight vehicle is determined by the use of the propulsion system model, adjusted with acceptance, preinstallation, and cold-flow test data for components of that particular vehicle. This method gives the most accurate data possible for use in mission planning, propellant budgeting, and other preflight activities.

A postflight analysis of the performance of the propulsion system during a mission is required to establish actual performance values in the flight environment and to identify and study instances of anomalous system behavior. Establishment of actual flight-system performance is required to evaluate the adequacy of the preflight prediction techniques. If necessary, the preflight models are updated, based on previous flight findings. The result is a continuing refinement in the prediction techniques, which leads to increased confidence in the capabilities of the propulsion system.

Identification and study of anomalous system behavior also are required to increase confidence in the capability of the propulsion system. Experience indicates that minor malfunctions and performance anomalies often exist; however, these malfunctions and anomalies have not, on any Apollo mission, precluded accomplishment of the mission on which they occurred. Even though these problems would not have prevented the accomplishment of a less than maximum mission, they could be indicators of subtle problems that would limit the capability of the vehicle to complete a maximum-capability

mission. Detection and resolution of these anomalies early in the flight test program are goals of postflight performance analysis efforts.

Once the models of the propulsion system are developed, numerous activities can be performed in support of the Apollo flights. Examples of this support are studies of the effect on system performance of various component malfunctions or of off-nominal system conditions, studies of backup or alternate missions, and definition of mission redline limits.

The importance of flight analysis support of the propulsion systems was recognized early in the Apollo Program, and efforts to develop the required capabilities were initiated. In this report, the ascent propulsion system (APS) is described, the techniques used to predict APS inflight performance and to determine inflight performance by postflight reconstruction are discussed, problems that have been encountered are discussed, and results derived from the analysis of APS performance during the Apollo 9, 10, and 11 missions are presented. Lunar module 3 (LM-3) was flown on the Apollo 9 mission, LM-4 on the Apollo 10 mission, and LM-5 on the Apollo 11 mission.

## DESCRIPTION OF THE ASCENT PROPULSION SYSTEM

### Hardware Description

The function of the APS is to provide the velocity ( $\Delta V$ ) necessary to take the ascent stage from the lunar surface into lunar orbit. The APS consists of a pressured, liquid-bipropellant, ablatively cooled rocket engine and its propellant feed, storage, and pressurization systems. A schematic of the APS is shown in figure 1.

The gaseous helium pressurant is stored in two spherical pressure vessels at a nominal initial pressure of  $2086 \text{ N/cm}^2$  (3025 psia) at ambient temperature. Prior to APS activation, each helium tank is isolated from the rest of the system by a squib-operated isolation valve. The helium tanks are manifolded to parallel helium flow paths, each of which contains a filter to trap any debris resulting from squib-valve actuation to prevent contamination of downstream components. After the filter, each helium flow path contains a normally open, latching solenoid valve and two pressure regulators.

The upstream regulators in each flow path are set to a slightly lower pressure than the respective downstream regulators, and the two series regulators in the primary flow path are set to a slightly higher pressure than the corresponding regulators in the secondary flow path. The pressure settings of the four regulators will vary from  $118.6$  to  $133.8 \text{ N/cm}^2$  (172 to 194 psi). The controlling regulator in the primary flow path is set at approximately  $126.9 \text{ N/cm}^2$  (184 psi).

In normal operation, the upstream regulator in the primary flow path is the controlling element; the downstream regulator senses the pressure in the outlet line and remains open because the sensed pressure is below the setting. The upstream



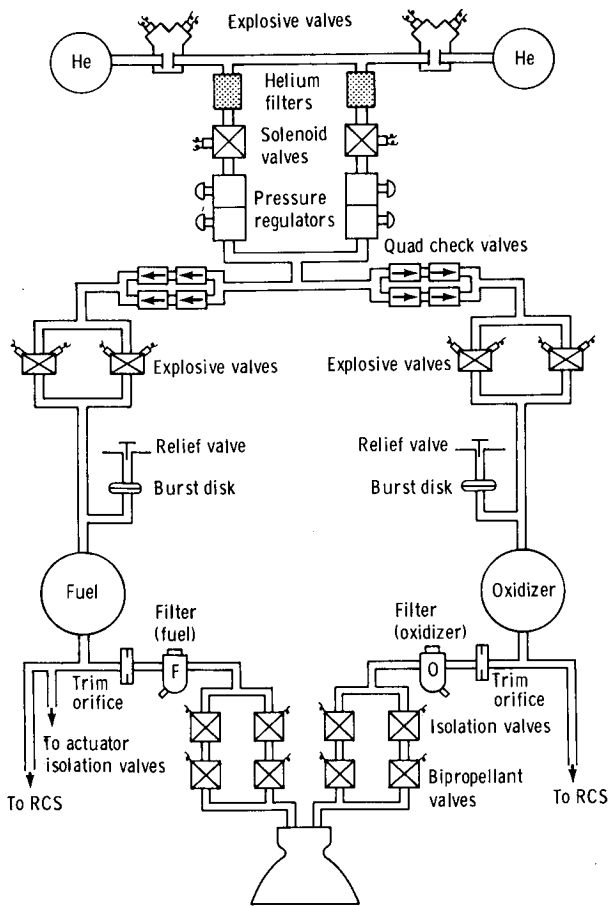


Figure 1. - Schematic of the APS.

simultaneously to initially pressurize the propellant tanks and feed system. A relief valve and its isolation burst disk are located in the helium pressurization line to each propellant tank to prevent catastrophic tank overpressurization. The APS propellant tanks do not have a quantity-gaging system but do contain low-level sensors that are used to provide an approximate 10-second warning of propellant depletion.

The APS contains one oxidizer tank and one fuel tank. The outflow from each tank divides into two paths. The main path leads through a trim orifice and a filter to the engine shutoff valves; the other path leads to normally closed solenoid valves interconnecting the APS and the reaction control system (RCS) propellant systems. Opening these valves permits the use of APS propellants by the RCS.

In addition, a flow path branches from the fuel side of the RCS interconnect line (upstream from the interconnect valve) and leads to the actuator isolation solenoid valves, which are arranged in parallel for purposes of redundancy. From the actuator isolation valves, the flow path goes to the four engine-actuator solenoid pilot valves. The purpose of these actuator isolation valves is to prevent possible fuel loss through leaking engine-actuator solenoid pilot valves before initial engine operation and during coast periods. The actuator isolation solenoid valves are opened and closed simultaneously with the engine-actuator solenoid pilot valves.

regulator in the secondary flow path is locked closed because its pressure demand is satisfied. If either regulator in the primary flow path fails to open, control is obtained through the regulator in the secondary flow path with the lower setting. If an upstream regulator fails to close, control is obtained through the downstream regulator of the same flow path. An open failure in a downstream regulator does not affect normal operation because the upstream regulator is already in control.

Downstream from the pressure regulators, the helium flow paths are manifolded together and divided into two separate propellant-tank pressurization paths, with a quadruple (quad) check valve in each. The function of the quad check valve is to prevent propellant liquid and vapor from the propellant tanks from backing up into the helium manifold. The quad arrangement provides series-parallel redundancy. Downstream of the quad check valves, in each flow path, are two normally closed squib valves arranged in parallel for redundancy. These valves provide a positive seal to prevent propellant vapors from diffusing through the quad check valves and into the common helium manifold. The helium-isolation squib valves are opened

The ascent engine consists primarily of an ablative-lined thrust chamber, an injector assembly, two propellant ducts and trim orifices, and a bipropellant valve assembly. The ascent engine is a constant-thrust, restartable engine, which develops a nominal 15 569 newtons (3500 pounds) of thrust in a vacuum. The engine is rigidly mounted to the ascent stage and oriented so that the thrust vector passes approximately through the center of gravity of the stage.

Propellant flow to the engine is controlled through the valve package, the trim orifices, and the injector. An expansion bellows is used in the feedlines between the valve package and the injector to accommodate the line expansion that results from the rise in injector temperature during engine firing. The valve assembly consists of similar propellant and isolation valves, mounted back to back, with oxidizer flow on one side and fuel flow on the other. This valve package contains a series-parallel arrangement of ball valves in fuel-oxidizer pairs. Each pair is simultaneously opened or closed on a common crankshaft by an actuator that uses fuel as the actuating medium. The fuel flow is controlled through the engine-actuator solenoid pilot valves. Nominal design and operating characteristics of the ascent engine are shown in table I.

TABLE I. - ASCENT-ENGINE DESIGN CHARACTERISTICS  
AND NOMINAL PERFORMANCE

Thrust, <sup>a</sup> N (lb) . . . . .	15 346 (3450)
Propellants:	
Oxidizer (O) . . . . .	Nitrogen tetroxide
Fuel (F) . . . . .	50-percent hydrazine/50-percent unsymmetrical dimethylhydra- zine
Mixture ratio, O/F . . . . .	1.6:1
Specific impulse, <sup>a</sup> sec . . . . .	309.7
Chamber pressure, N/cm <sup>2</sup> (psia) . . . . .	84.8 (123)
Propellant flow rate, kg/sec (lb/sec) . . . . .	5.08 (11.2)
Expansion-area ratio . . . . .	45.6:1

<sup>a</sup>These values were determined as typical of the class of C-series Rocketdyne engines when fired for a nominal (460 second) duty cycle.

## Instrumentation Description

Transducers and position sensors located throughout the APS are used to measure temperatures, pressures, quantities, and valve positions. The sensor locations in the system and the obtained data are described in figure 2. The parameters listed in figure 2 are the data available on all lunar modules with operational instrumentation (LM-4 and subsequent vehicles). All operational-instrumentation data are telemetered using pulse code modulation (PCM). Sensor ranges, accuracy levels, and sample rates for the operational instrumentation are given in table II.

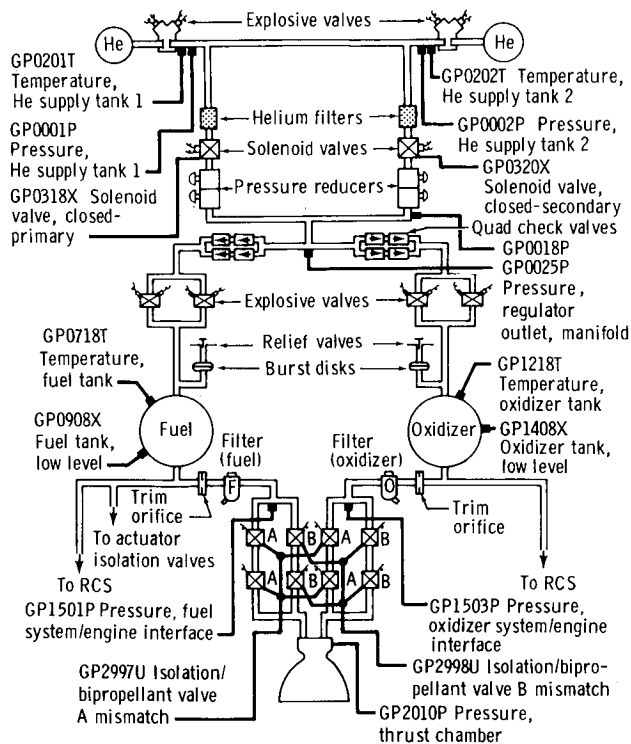


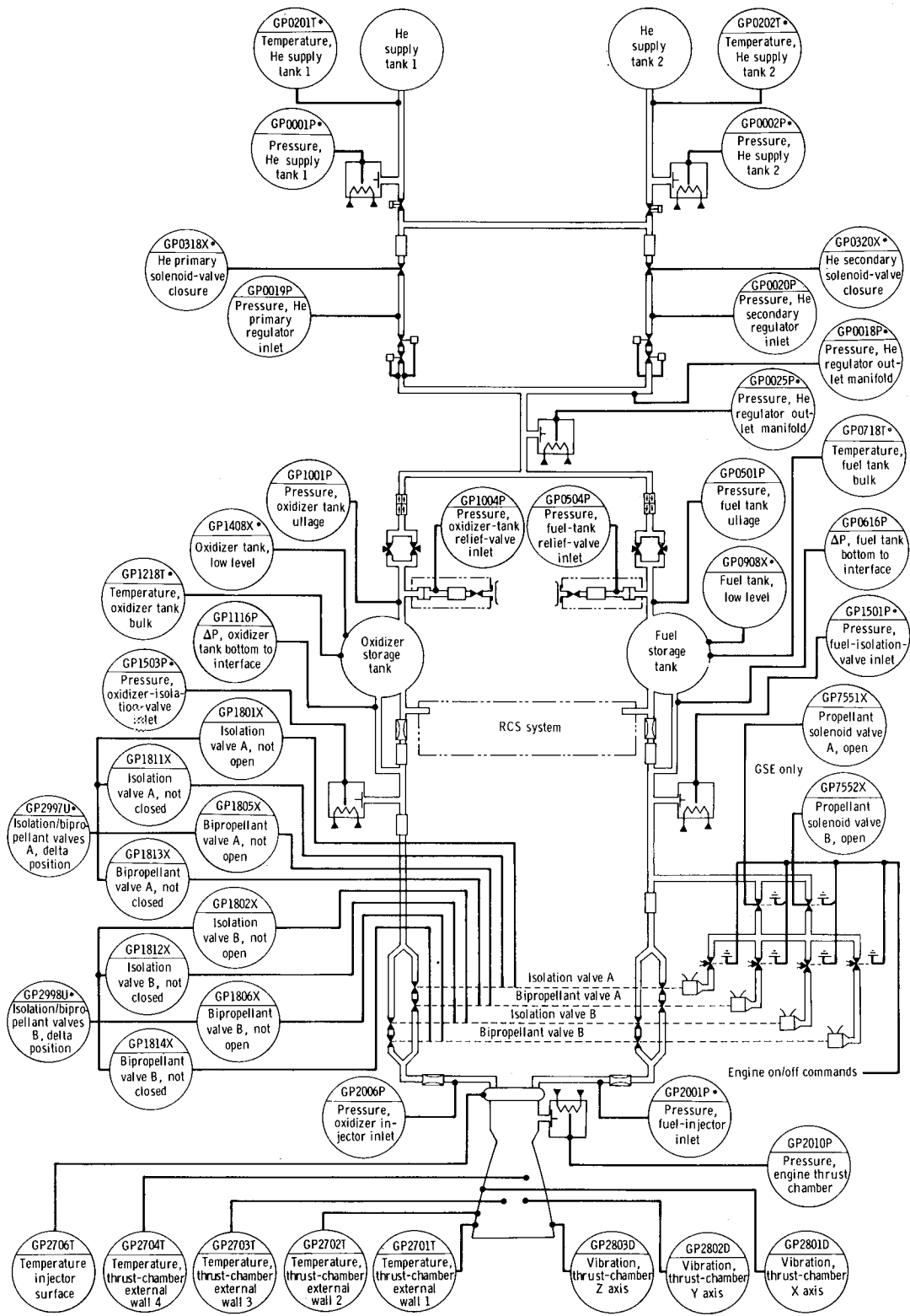
Figure 2. - Real-time telemetry (PCM) of the APS.

In addition to the operational instrumentation, the LM-3 vehicle was equipped with developmental flight instrumentation (DFI). The purpose of this additional instrumentation was to allow more accurate postflight analysis of the operation and performance of the LM subsystems on early flights. The operational and DFI instrumentation data available on the LM-3 APS are illustrated in figure 3. The DFI data are telemetered as continuous analog data (FM/FM) or as pulse-amplitude-modulated data.

The vehicle-acceleration data derived from the LM guidance computer (LGC) output, although not part of the APS, is an additional quantity that is an important measurement for determination of APS performance. The LGC receives inputs from the pulse-integrating pendulous accelerometers. The LGC processes these data and outputs the change in velocity experienced by the vehicle (in each of the axes) over a 2-second timespan.

TABLE II. - ASCENT PROPULSION SYSTEM OPERATIONAL INSTRUMENTATION

Measurement number	Description	Range	Sample rate, samples/sec	Accuracy, percent
GP0001P	Pressure, helium tank 1	0 to 2758 N/cm <sup>2</sup> (0 to 4000 psia)	1	2.9
GP0002P	Pressure, helium tank 2	0 to 2758 N/cm <sup>2</sup> (0 to 4000 psia)	1	2.9
GP0018P	Pressure, secondary regulator outlet	0 to 207 N/cm <sup>2</sup> (0 to 300 psia)	1	2.0
GP0025P	Pressure, primary regulator outlet	0 to 207 N/cm <sup>2</sup> (0 to 300 psia)	1	2.0
GP0201T	Temperature, helium tank 1	144° to 367° K (-200° to +200° F)	1	1.7
GP0202T	Temperature, helium tank 2	144° to 367° K (-200° to +200° F)	1	1.7
GP0318X	Helium primary solenoid valve	Open/closed	1	--
GP0320X	Helium secondary solenoid valve	Open/closed	1	--
GP0718T	Temperature, fuel bulk	267° to 322° K (20° to 120° F)	1	2.8
GP0908X	Fuel, low level	On/off	1	--
GP1218T	Temperature, oxidizer bulk	267° to 322° K (20° to 120° F)	1	2.8
GP1408X	Oxidizer, low level	On/off	1	--
GP2010P	Pressure, thrust chamber	0 to 103.4 N/cm <sup>2</sup> (0 to 150 psia)	200	2.1
GP2997U	Isolation/bipropellant valves A, delta position	On/off	1	--
GP2998U	Isolation/bipropellant valve B, delta position	On/off	1	--
GH1230	Ascent-engine arming switch	On/off	50	--
GH1260	Ascent-engine switch, on/off	On/off	50	--
GP1501P	Pressure, fuel-isolation-valve inlet	0 to 172.3 N/cm <sup>2</sup> (0 to 250 psia)	1	2.2
GP1503P	Pressure, oxidizer-isolation-valve inlet	0 to 172.3 N/cm <sup>2</sup> (0 to 250 psia)	1	2.2



\* = PCM  
 GSE = ground support equipment

Figure 3. - Telemetry (PCM and DFI) of the APS.

## PREFLIGHT ANALYSIS ACTIVITIES

Because the APS is not static fired as a complete system before flight, the flight-performance prediction must be derived from test data of the individual components and models of the APS involving theoretical, empirical, and empirically adjusted theoretical equations. These equations form the mathematical model of the APS used in the propulsion-analysis trajectory-simulation (PATS) computer program, which is used to simulate the mission of the APS and to analyze the performance of the APS.

Studies to determine the uncertainties associated with the predicted performance values also are performed as a portion of preflight analysis activities. Test-facility instrumentation, the lack of hardware repeatability, and characterization-equation uncertainties are included in these analyses.

Additionally, malfunction studies and other special data requests are done as a part of preflight analysis activities. In these cases, the APS model is used to simulate the effects of various component malfunctions or specified off-nominal conditions. The operations and data flow involved in preflight simulation are illustrated in figure 4.

### Program and Model Description

The primary analytical tool employed in performing a preflight performance prediction is the computer program used to simulate the operation of the APS over the desired mission duty cycle. The program used for this purpose is the PATS program (ref. 1). The PATS program is a generalized, two-dimensional, point-mass trajectory program.

Propulsion-analysis trajectory-simulation program. - The basic PATS program contains simulations of vehicle propellant feed system and engine system and uses a two-dimensional trajectory calculation that includes aerodynamic normal and axial forces. The nonlinear model of the liquid-bipropellant engine and feed system is capable of simulating pressure-fed propulsion systems with both fixed and variable thrusts.

A search option exists in PATS that uses parameter matching routines to determine a set of independent variable values that will achieve a specified set of

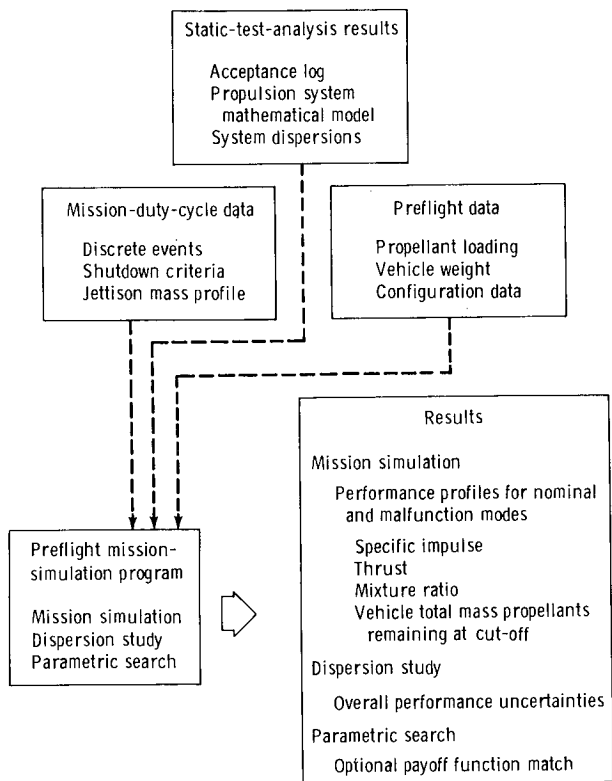


Figure 4. - Preflight mission-simulation input/output.

dependent variable values. The solution is a minimum-error analysis (using a Newton-Raphson iteration) so that the capability exists to solve overdetermined or underdetermined problems (number of equations larger or smaller than the number of unknowns). Also, this capability may be used to find the extremum of functions.

Ascent propulsion system model. - To provide an accurate simulation of the APS, it was necessary to expand the capabilities of the original propulsion system model used by PATS. The capabilities and significant features of the present APS model are discussed in the following paragraphs.

The pressurization system of the APS does not include a method of conditioning the helium to a constant temperature before introducing it into the propellant tanks. Thus, as an APS burn continues, expansion of the helium in the storage tanks leads to progressively colder helium inlet temperatures to the propellant-tank ullage space. A system of this type requires more effort to model than the case in which a helium heat exchanger is used because the constantly changing temperature of the helium must be calculated to predict helium requirements accurately.

A generalized model of a two-tank, ambiently stored, noncondensable-gas pressurization system is used. Convection heat-transfer rates between the helium in the storage tanks and the tank walls are calculated by use of the lumped-parameter method. The helium supply lines and line components are broken into nodes, and heat-transfer rates between these nodes and the flowing helium are calculated; the tanks and lines are considered adiabatic with respect to the surroundings. Also, the model calculates the Joule-Thomson heating that occurs in the helium regulators. The helium flow rates are calculated on the basis of the pressure difference between the regulator outlet and the propellant-tank ullage. Also, the pressure drop experienced by the helium in the supply lines and check valves is calculated.

Another area of concern in predicting helium requirements for the APS is in the simulation of the heat transfer and other thermodynamic processes occurring in the propellant-tank ullage space. In the APS model, heat transfer is considered to occur between the pressurant and the liquid propellant, between the ullage gases and the propellant-tank wall, and between the propellant-tank wall and the liquid propellant. Heat transfer caused by pressurant-gas inflow and ullage-gas venting is considered. Also, the model considers the heat and mass transfer resulting from propellant-vapor dissociation, surface condensation or evaporation at the ullage-gas liquid-propellant interface, condensation of propellant vapor at the tank wall, and cloud condensation of propellant vapor from the ullage. All of these calculations are made assuming lumped-mass systems except for the propellant-tank wall, which is composed of two nodes (one in contact with the ullage and the other in contact with the liquid propellant).

The pressure drop in the propellant feedlines is calculated with the use of a fluid-flow resistance value. This resistance value includes the pressure drops caused by flow in the feedlines and by the balancing orifices installed in the feedlines.

To this point, the model has calculated all necessary parameters upstream from the engine. With the propellant conditions at the interface of the engine feed system known as a function of values for propellant flow rate, the nonlinear engine model, using an engine-performance characterization, performs an iterative balance

procedure<sup>1</sup> to determine the engine operating conditions and the performance as a function of the upstream conditions previously calculated.

The engine characterization consists of characteristic exhaust velocity  $C^*$ ; thrust coefficient  $C_F$ ; throat area  $A_t$ ; interface-to-chamber fluid-flow resistances, which are defined as functions of their respective values measured during sea level and altitude acceptance testing; and, where applicable, predicted values of chamber pressure  $P_c$ , mixture ratio  $\mu$ , propellant temperature  $T$ , engine burn time  $t_b$ , and accumulated time on chamber  $t_{acc}$ .

## Data Acquisition and Treatment

Much data must be obtained to perform an APS preflight performance analysis. This body of data includes basic characterization data such as those resulting from ground testing of propulsion system components and of propulsion system test articles as well as the definition of physical characteristics of the system such as propellant-tank and feedline geometries. Also included are acceptance test data detailing the performance expected from a particular component or system, and mission-related data such as mission profiles, mass properties, and vehicle thermal analyses. The basic characterization data are used to construct, refine, and verify the models of the propulsion system. The acceptance test data provide inputs to tailor the model to a particular vehicle. Other inputs such as the mission duty cycle, vehicle weights, and propellant temperatures are obtained from the mission-related preflight data.

System-characterization data. - Much of the APS mathematical model is composed of theoretically based characterizations of the performance of the various components as a function of their operating conditions. In some cases, the theoretical characterizations have been adequate representations; for other components, the theoretical characterizations have been modified by empirically determined coefficients. For other components for which no theoretical characterization is available, the characterizations are wholly empirical.

Ground test data used to develop and verify the PATS APS model were obtained from many sources, including the NASA Lyndon B. Johnson Space Center (JSC), formerly the NASA Manned Spacecraft Center (MSC), White Sands Test Facility (WSTF), the Grumman Aerospace Corporation (GAC), and Rocketdyne Division of North American Rockwell (Rocketdyne). The WSTF test was concerned primarily with

---

<sup>1</sup>The problem of finding pressures and flow rates that satisfy the equations describing the steady-state operation of a liquid-fueled rocket engine is called the engine-balance problem. These equations are nonlinear and are implicit in the desired variables. The term balance arises from the fact that one must perturbate and balance equations representing two different fluid-dynamic processes (viscous, incompressible fluid dynamics in the propellant feed system and gas dynamics in the engine) to agree simultaneously upon the quantities of flow rate and chamber pressure. Also, the effect of acceleration head on the propellant inlet pressures must be taken into account in the balance procedure.



cold-flow and hot-firing tests of the prototype ascent feed system. The GAC testing included preinstallation testing (PIT) of various components and cold-flow testing of flight LM vehicles (with substitute propellants). The testing at Rocketdyne was concerned with development of the ascent engine.

Examples of the data used from these facilities or tests are as follows.

1. From WSTF: correlation between substitute and actual propellant cold-flow results, which allowed use of the cold-flow data from GAC, and evaluation of propellant-tank ullage and liquid temperatures during an engine firing
2. From GAC: cold-flow (substitute propellant) results for LM flight vehicles
3. From PIT: data for components such as helium regulators and check valves
4. From Rocketdyne: engine-performance data, ablative-chamber erosion-rate data, and fluid-flow resistances of the engine

Data of this type are required for an APS model that is sufficiently accurate to allow meaningful results to be obtained.

Acceptance test data. - Because of uncontrollable variabilities, which will inevitably exist in any hardware system, the APS characterization must be adjusted to reflect the performance of each vehicle. The primary areas where this variability is considered are in the fluid-flow resistances of the propellant feedlines and the performance level, throat area, and fluid-flow resistances of the engine.

The best estimate of the steady-state inflight performance of the ascent engine is obtained by using a combination of sea-level and altitude engine-acceptance-test data. Values obtained from acceptance test data include characteristic exhaust velocity  $C^*$ , mixture ratio, specific impulse  $I_{sp}$ , chamber pressure, accumulated chamber burn time, and fuel and oxidizer flow resistances. Data obtained from sea-level testing are used to calculate  $C^*$  because of the water-cooled throat used on the engine during sea-level testing. This engine configuration produces more repeatable  $C^*$  values than are obtained at altitude. The sea-level  $C^*$  is modified by a factor derived by Rocketdyne from data obtained from ascent-engine testing (17 engines) to account for the difference between the water-cooled throat/ablative liner used at sea level and the actual flight ablative chamber used at altitude. The characterization input value for  $I_{sp}$  is obtained from altitude acceptance test data by adjusting the observed engine  $I_{sp}$  to account for a degradation in  $I_{sp}$  from firing to firing. The magnitude of this degradation has been calculated to be 0.3 second of  $I_{sp}$  for each firing, and, although no physical explanation of this degradation is available, it is substantiated by considerable test data obtained during ground testing at Rocketdyne. The accumulated burn time on the chamber is a parameter because the change of  $I_{sp}$  with time during a burn, the erosion rate of the engine throat, and the fluid-flow resistance have been found to be functions of preflight burn time accumulated on the chamber.

Mission-related data. - The mission-related data are required to tailor the simulation to a specific mission and vehicle. The data include items such as mission profiles, mass properties, and vehicle thermal analyses. The mission profile, which is a timeline of the mission, gives active and inactive periods and the burn and coast schedules of the propulsion system. Mass-properties data define the vehicle weight and propellant quantities at specific points in the mission. A vehicle thermal analysis, performed using a given mission profile, yields information concerning the expected temperatures of propellants and pressurants at the start of the APS burn.

These data define the initial conditions for the APS at the start of the burn that is to be simulated. In addition, the mission profile defines the  $\Delta V$  required from the APS.

## Preflight Performance Analysis

Basically, the preflight performance analysis consists of simulating the particular mission with the use of the PATS program, analyzing the dispersions on the primary output quantities, and publishing the results obtained as a supplement to the MSC Spacecraft Operational Data Book (SODB). These results, defining the performance values expected from the APS under the conditions used in the simulation, are used by other MSC organizations in simulation of the entire mission to perform  $\Delta V$  and propellant-budget analyses and are used to define, for real-time mission-support personnel, the values of the APS measurements expected during the mission.

Mission simulation. - For the APS, a mission simulation consists of determining the expected initial conditions at the start of the APS burn and, with these conditions as input to the PATS program (in addition to the other data discussed previously), simulating the mission duty cycle of the APS with PATS. The PATS output has the form of a digital printout and a digital tape. This output includes parameters such as pressure and temperature histories simulating APS measurements, and derived parameters such as thrust, mixture ratio, and specific impulse.

The expected initial conditions are determined by taking target loading values for propellant and helium, and using thermal analysis results, predicted helium-solubility effects, and the effect of prefire pressurization of the propellant tanks to define the state of the fluids in the propellant and helium tanks at the beginning of the APS burn. Other inputs are derived from acceptance test and functional-checkout results. These values include feed system and engine fluid-flow resistances, helium-regulator outlet pressure, and engine-performance parameters such as characteristic exhaust velocity and specific impulse.

When input to the PATS, the data just discussed establish the state of the APS at the initial time point of the duty cycle being simulated. The PATS program uses the APS model to determine time derivatives of the state of the system. These derivatives are used to integrate the state of the system ahead to a new time point, where the process is repeated. This procedure continues until the entire burn has been simulated.

A complicating factor in predicting APS performance is the RCS usage of propellant from the APS tanks through the APS/RCS interconnect. The interconnect is normally open during the ascent burn (for which RCS attitude control is necessary because

of the fixed mounting of the ascent engine) to conserve the RCS propellant stored in the dedicated RCS tanks. For the earlier APS preflight simulations, estimates of expected RCS interconnect usage were obtained and incorporated into the APS simulation; however, it became evident that a more satisfactory procedure was to neglect the RCS effects. This method lessened the potential for misunderstanding and increased the flexibility of the mission-planning personnel concerned with mission simulation and propellant budgeting.

The output obtained from PATS includes a digital printout of significant parameters at a selected time interval. This printout is used for checks on the validity of the input data used in the simulation and for determining precise values of a given parameter at a specific time, if required. The most useful form of output from PATS is a digital tape that contains selected parameters at every time point. This tape is processed by various auxiliary programs to yield values of parameters of interest averaged over the burn and plots showing the variation in the parameters as a function of time.

Dispersion studies. - The studies made to determine the magnitude of the uncertainty bands associated with the preflight-predicted APS performance values are an important part of the preflight analysis activities. The APS uncertainties result from several sources, including the following: the lack of hardware repeatability, instrumentation uncertainty, uncertainties in prediction of the state of the system at the beginning of the mission duty cycle, and uncertainties in the APS model. Accurate knowledge of the APS dispersions is important so that the probability of attaining a particular mission objective can be determined. For example, if a particular vehicle velocity requirement is based on predicted APS performance and payload requirements, the variability in propulsion performance may not indicate a sufficiently high probability that the predicted performance will be attained. The usual procedure is to load an additional amount of propellant (reserves) based on the probability that vehicle performance, including that of the propulsion system, will be less than predicted. If a vehicle performs as predicted, the reserves will not be consumed, and the additional propellant weight represents a decrease in payload capability. Part of the variability of a system is inherent in the system hardware and cannot be improved without design changes; however, a substantial amount of the variability represents a lack of confidence in the capability to predict system performance. Thus, improved analysis techniques, both system modeling and dispersion analyses, may often afford greater payload potential by decreasing propellant reserve requirements.

The PATS program is used to determine the effect of dispersions in the input independent variables, such as propellant temperature, ullage pressure, and propellant-feed-system resistance, on the calculated dependent variables, such as engine thrust, specific impulse, and mixture ratio. The resultant perturbations in the dependent parameters are then root sum squared to determine the uncertainties associated with the calculated dependent parameters. Typical values used as input to PATS and the results obtained are illustrated in table III. The general approach and techniques used in the calculation of propulsion system dispersions are discussed in detail in reference 2.

TABLE III. - TYPICAL VALUES USED IN THE CALCULATION  
OF APS PERFORMANCE DISPERSIONS

Parameter	3 $\sigma$
Input uncertainties	
Characteristic exhaust velocity C*, m/sec (ft/sec) . . . . .	18.83 (61.8)
Specific impulse I <sub>sp</sub> , sec . . . . .	3.50
Mixture ratio, O/F . . . . .	.029
Propellant-feed-system oxidizer resistance, N-sec <sup>2</sup> /kg-m <sup>5</sup> (lb <sub>f</sub> -sec <sup>2</sup> /lb <sub>m</sub> -ft <sup>5</sup> ) . . . . .	.00788 (29.37)
Propellant-feed-system fuel resistance, N-sec <sup>2</sup> /kg-m <sup>5</sup> (lb <sub>f</sub> -sec <sup>2</sup> /lb <sub>m</sub> -ft <sup>5</sup> ) . . . . .	.0103 (38.4)
Propellant-tank ullage pressures, N/cm <sup>2</sup> (psia) . . . . .	2.76 (4.0)
Propellant-tank ullage pressure differential ( $\Delta P$ ), N/cm <sup>2</sup> (psia) . . . . .	.344 (.5)
Propellant bulk temperatures, °K (°F) . . . . .	2.78 (5.0)
Propellant bulk temperature differential ( $\Delta T$ ), °K (°F) . . . . .	.83 (1.5)
Ablative engine-throat area, cm <sup>2</sup> (in <sup>2</sup> ) . . . . .	4.12 (.639)
Output dispersions	
Specific impulse, sec . . . . .	3.50
Thrust, N (lb <sub>f</sub> ) . . . . .	458.2 (103.0)
Mixture ratio, O/F . . . . .	.026

## Malfunction Simulations and Special Data Requests

The PATS simulations of APS performance have been made to evaluate the effect of hardware malfunctions, off-nominal environmental conditions, and other types of off-nominal system operation. Simulations of this type illustrate the value of having a propulsion system model that is closely related to the physical characteristics of the system, as opposed to an influence coefficient propulsion model.

The ascent propulsion system malfunction/off-nominal operation simulations that have been performed to date include the following: high engine-throat erosion, off-nominal helium-regulator outlet pressure, off-nominal propellant temperatures (oxidizer and fuel together, with a temperature differential ( $\Delta T$ ) between oxidizer and fuel), and unbalanced ullage pressures. The effect of the conditions listed previously on APS performance has been determined by PATS simulation. The values obtained from these simulations are illustrated in figures 5 and 6, which represent the change in engine performance caused by off-nominal temperatures of propellants that are saturated with helium and of nonsaturated propellants. A summary of the calculated effects for the list of off-nominal operational conditions is presented in table IV.

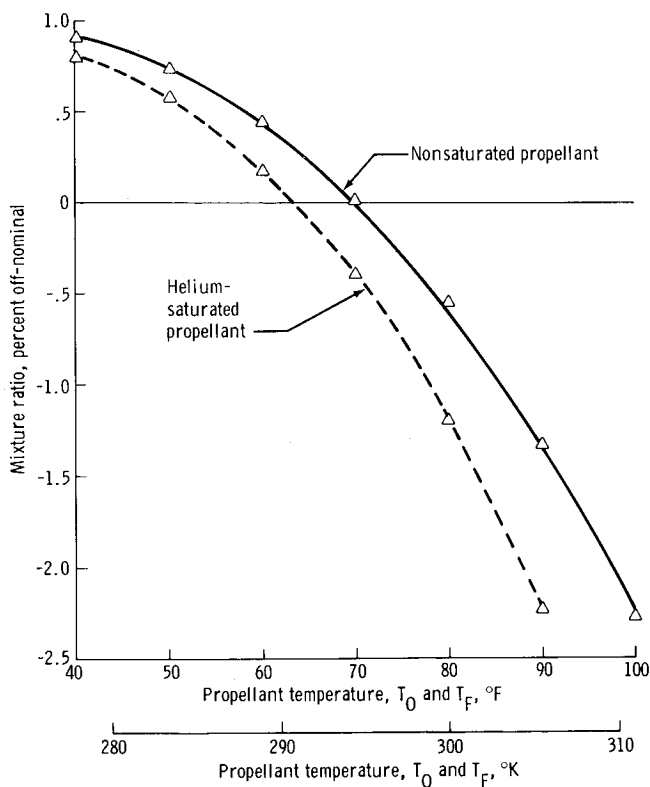


Figure 5. - Effect of propellant temperature on APS mixture ratio.

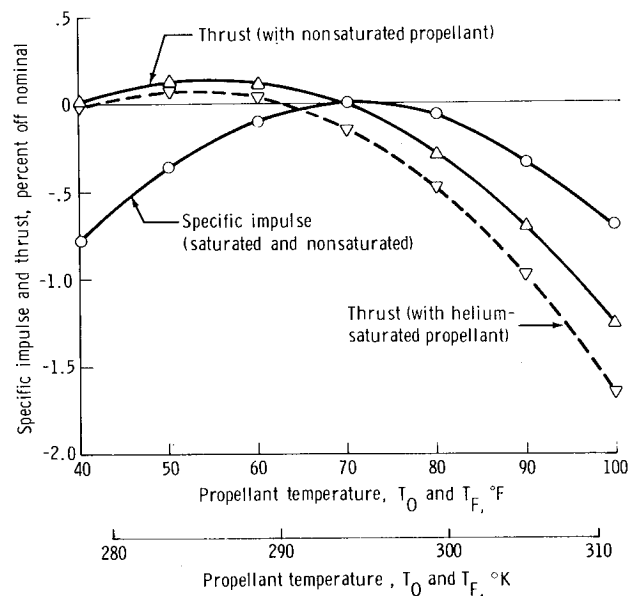


Figure 6. - Effect of propellant temperature on APS engine thrust and specific impulse.

TABLE IV. - EFFECT OF VARIOUS MALFUNCTIONS  
ON APS PERFORMANCE VALUES

Off-nominal condition	Effect on APS performance <sup>a</sup>		
	I <sub>sp</sub> , sec	Thrust, N (lb <sub>f</sub> )	Mixture ratio, O/F
Engine-valve failure	0	-334 (-75)	-0.022
High engine-throat erosion (8 percent greater than nominal)	-.9	+329 (+74)	0
High helium-regulator outlet pressure (5.5 N/cm <sup>2</sup> (+8 psi) from nominal)	0	+712 (+160)	0
Low helium-regulator outlet pressure (-10.3 N/cm <sup>2</sup> (-15 psi) from nominal)	0	-979 (-220)	0
High propellant temperature (311° K (100° F))	-2.1	-236 (-53)	-.047
Low propellant temperature (278° K (40° F))	-2.4	0	+.018
Mismatched propellant temperatures (oxidizer, 289° K (60° F); fuel, 294° K (70° F))	0	0	+.005
Imbalanced interface pressures (oxidizer, 117 N/cm <sup>2</sup> (170 psia); fuel, 110 N/cm <sup>2</sup> (160 psia))	-1.2	-258 (-58)	+.207

<sup>a</sup>Mission-duty-cycle average values.

## POSTFLIGHT ANALYSIS ACTIVITIES

Development of the postflight analysis tools and techniques was begun with the goal of performing real-time or near-real-time analysis of the propulsion system performance. The inflight analysis of the propulsion system performance would use propulsion and trajectory data telemetered and reduced in real time to evaluate propulsion firings in a postevent fashion. The final results of the analysis, which would lag the actual event by only a few minutes, were to include the following: an accurate determination of subsystem performance, malfunction detection and resolution, and an accurate prediction of subsystem performance later in the mission. These results would be used to reevaluate the mission plan and, if necessary, select possible alternatives. This information would be supplied to the flight controllers who formulate inflight

decisions. Although this scheme was not accomplished, it formed the basis for the methods now used for postflight determination of propulsion system performance.

The postflight analysis effort is a more sophisticated and detailed version of the originally proposed inflight analysis. All available flight data are used in the reconstruction of the mission and the evaluation of the propulsion system performance. The results of these analyses are used to establish propulsion system performance, to identify and evaluate system malfunctions, and to update the preflight prediction models and techniques as required. The overall primary objective is information feedback of actual inflight performance data into the system developmental programs and future mission planning.

## Program and Model Description

The postflight analysis effort requires a method of determining, from flight data, estimates of propulsion system performance of sufficient accuracy to allow for the evaluation and refinement of preflight predictions. In addition, the postflight analysis method must incorporate a simulation of the propulsion system to compare preflight estimates of system performance with performance calculated from the flight data. Because the flight data and the preflight estimates contain errors of a statistical type, a statistical technique must be employed in the analysis.

Apollo propulsion analysis program. - The preceding requirements are met by a computer program known as the Apollo propulsion analysis program (APAP). An earlier version of APAP, a program known as ORACLE-MAFIA, is described in considerable detail in reference 3. Both APAP and ORACLE-MAFIA have essentially the same mathematical formulations. The primary difference between the two is that APAP incorporates a preprocessor, known as the model compiler (MC), which greatly simplifies program use.

The APAP is programed to solve three mathematical problems: integration of differential equations, for which the user must specify the equations to calculate the derivatives; minimum-variance estimation (MVE) using measured data, for which the user must specify equations to calculate estimates of the measurements; and solution of nonlinear, implicit, simultaneous equations, for which the user must specify the equations and the independent variables. All of these capabilities are used in propulsion system performance analysis.

The program is designed to be general because only the mathematics of the numerical solution is fixed; that is, the mathematical model of the system being analyzed is input to the program. Thus, the program is not limited to analysis of propulsion systems but is adaptable to other types of systems. These systems may be described by either linear or nonlinear equations. An iterative scheme is incorporated to allow consideration of nonlinear systems.

A basic premise of APAP is that no data are perfect. The data used in deriving the system mathematical models and the flight test data contain statistical errors, and each data source (such as pressure transducers and guidance system) has a different uncertainty associated with it. Thus, the basic mathematical approach employed for

postflight analysis is a technique known as minimum-variance estimation, involving weighted least squares; that is, it is desired to minimize a function of the form

$$\chi^2 = \sum_{i=1}^m \sum_{j=1}^n \frac{(y_{ij}^* - \hat{y}_{ij})^2}{\sigma_{ij}^2} \quad (1)$$

where  $y_{ij}^*$  = a measured data value

$\hat{y}_{ij}$  = an estimate calculated by the system model of the data value  $y_{ij}^*$

$\sigma_{ij}$  = an a priori estimate of the standard deviation of the data point (including uncertainties in the model and in the data)

$m$  = the number of measurements used

$n$  = the number of data points per measurement

This technique allows the calculation of the best (from a statistical standpoint) estimate of the pertinent propulsion system parameters from applicable test data.

The APAP provides an MVE of the state variables of the system ( $X$ ) by applying a minimum-variance estimator to the dependent measurement variables ( $y$ ), the estimates of which can be computed from the state variables. The state variables are related to one another in time by a system of differential equations. The governing equations are

$$\frac{dX_j}{dt} = f_j(X_1, X_2, \dots, X_m) \quad j = 1, 2, \dots, m \quad (2)$$

where  $m$  = the number of independent variables

and

$$y_i(t) = g_i(X_1, X_2, \dots, X_m) \quad i = 1, 2, \dots, n \quad (3)$$

where  $n$  = the number of measurement variables.

Estimated measurement values  $\hat{y}_i$  are calculated from the functions  $y_i(t)$  and are used in the MVE to obtain improved estimates of the state  $X_j$ . The mathematical



model of the system is used to compute the functions  $f_j$  and  $g_i$  and several partial derivative matrices required in the solution. Given these quantities and actual system data measurements  $y_i^*$ , the program will calculate an MVE of the initial state vector  $X_0$ .

The solution requires several partial derivative matrices. This requirement is typical of many algorithms in the field of systems analysis and has presented an obstacle known to the implementation of desirable mathematical schemes. Several methods of supplying the required partial derivative matrices are available.

1. Programing the required partial derivatives along with the system model is probably the most accurate and the most expeditious method for the computer; however, it requires a large effort by the user (in formulating and programing the derivatives), makes even a simple model large and difficult to debug, and renders changes to the model a difficult and time-consuming task.

2. Calculation of the derivatives numerically within the program greatly simplifies the system model and provides a dramatic decrease in the burden on the user. The principal drawback is the loss of accuracy inherent in a numerical differentiation process; double precision calculations probably will be required, and even this step may not reduce the errors to an acceptable level.

3. Automatic generation of analytical partial derivatives combines the accuracy of the first method and the simplicity and flexibility of the second. The algorithm used to perform these operations was developed within MSC.

This algorithm was developed into a processor known as the model compiler (MC). The MC acts as a symbolic input processor to calculate specified partial derivatives from the alphanumeric input (FORTRAN) expressions comprising the system model. The MC performs a lexical analysis of the FORTRAN expression and breaks the expression into a string of basic operations (addition, multiplication, exponentiation, et cetera), the differentials of which are preprogramed. These derivatives are combined, using the chain rule to obtain the desired derivatives of the original expression. A description of the MC is found in reference 4.

Ascent propulsion system model. - The mathematical model of the APS used in APAP is essentially the same as that used in PATS, with several exceptions caused by the different nature of the two programs. In the construction of a propulsion system model, the starting point or driving potential must be selected. The helium pressurization system is the logical choice for the starting point because the helium pressure is the actual driving potential of the system. The APS model used in PATS is constructed in this manner. However, when the pressurization system is included, the propulsion system model becomes somewhat large. In addition, a precise characterization of the helium pressure regulators is difficult. A more satisfactory approach for APAP has been to model only the engine, feed system, and propellant tanks, and to drive the model from the system-engine interface pressure data. A model has been developed that uses helium-regulator outlet pressure as the driver, but this model has not been employed in establishing any of the results presented in this paper.

Driving the model with interface pressures does not mean that upstream pressure measurements are ignored. The model begins at the interface, calculates values downstream to the chamber pressure, and establishes an engine balance between the hydraulics of the feed system and the gas dynamics of the combustion chamber. After this balance is achieved, calculations are performed from the interface upstream to the propellant-tank pressures and feedline pressure change ( $\Delta P$ ), where available, and to the helium-regulator outlet pressure. Thus, comparisons are made in the program between model-predicted pressures in the system and flight results.

When the model is driven by flight pressures (interface pressure measurements), the program is allowed to follow the exhibited trends or pressure profiles. The program is not constrained to the absolute magnitudes of the measurements and can adjust or bias the measurements up or down, as necessary, to obtain the best overall fit to the data. This technique makes practical sense because a transducer does not necessarily measure exactly the absolute value but can be expected to provide an accurate indication of trends. Consequently, the program is using the best information provided by the instrumentation (pressure trends instead of the absolute-pressure magnitudes).

## Data Acquisition and Treatment

The data used in the postflight performance analysis are from ground testing and flight testing. The ground test data provide the mathematical models, the predicted system performance parameters, and the dispersions of the parameters. Activities relating to acquisition and treatment of ground test data were discussed earlier. The flight test data provide information by which the performance parameters and coefficients in the model are adjusted to determine the actual performance in flight.

Flight-data acquisition. - To monitor flights in real time, MSC receives flight data of critical measurements at a reduced sample rate. After the flight is concluded, the station tapes, containing the full sample-rate data recorded at remote telemetry stations, are delivered to MSC. These data are processed at MSC to convert the data from the PCM analog to a PCM digital format. The data are quantified (converted to engineering units) and delivered to the personnel responsible for the propulsion system analysis.

At this point, the tapes are known as raw data tapes. These data are plotted for qualitative examination and study of transient behavior. The data to be used for APAP analysis is wild-point edited and smoothed with an orthogonal-polynomial, sliding-arc filter. The smoothed data then are sliced at a sample rate suitable for input to the analysis program. Also, the smoothed data are plotted after all processing is complete, primarily to verify that the operations have been conducted properly.

In addition, the  $\Delta V$  data from the LGC are specially processed. These data, which are in the form of velocity increment counts, are edited to eliminate bad data and then are scaled, biased, smoothed, sliced, and converted to accelerations. The acceleration data are merged with the smoothed propulsion system data. The resultant tape is the input to the analysis program. The flow for the processing of propulsion system flight data is shown in figure 7.

PGNS = Primary Guidance and Navigation System  
 CAAD = Computation and Analysis Division  
 E & D = Engineering and Development (Directorate)  
 SEEACC, SIMUPLOT, TEDIT = computer programs for data processing

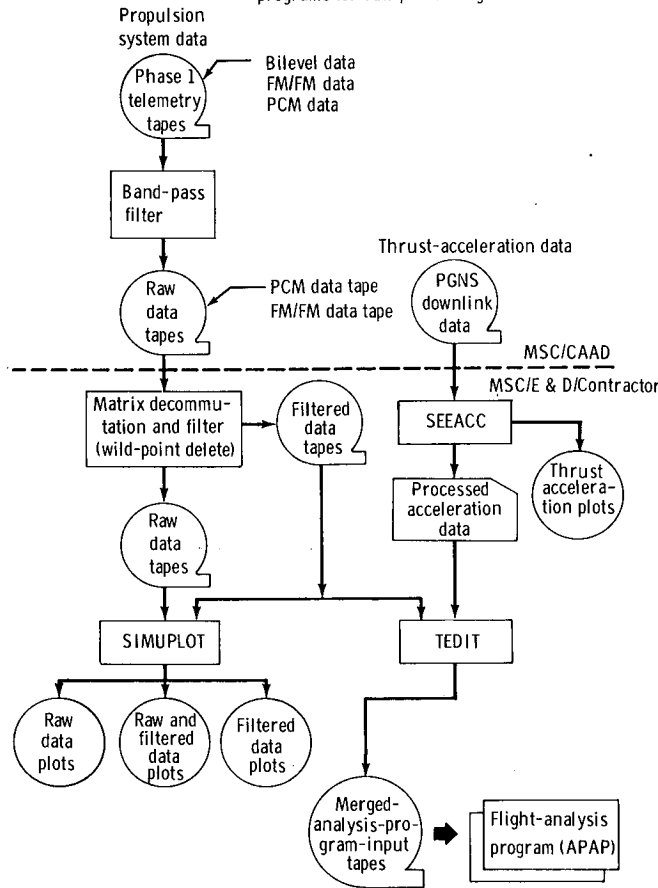


Figure 7. - Postflight data-flow logic diagram.

**Data classification.** - The data used for analysis of Apollo flights may be divided into three classes: class 1 data (statistically matched constraints), class 2 data (imposed flight test or ground test data from the hardware flown), and class 3 data (standard spacecraft parameters).

Class 1 data, matched statistically in an MVE sense, consist of the following items: thrust-acceleration history; vehicle damp weight; loaded oxidizer and fuel/propellant weights; propellant volumes on board at discrete times; pressure profiles of the propellant feed system and engine; internal resistances of propellant feedline and engine; and thrust-chamber throat area, characteristic velocity  $C^*$ , or thrust coefficient  $C_f$  (any two but not all three, the best set being dependent on the particular analysis).

Class 2 data are those observed from the flight hardware. The data are used as input to the program and are not adjusted by the program. Class 2 data consist of the following items: engine start and cut-off times; propellant-density time histories (from temperature measurements, et cetera); propellant-ullage or interface-pressure time histories (depending on the set used for the specific flight); thrust-chamber throat area, characteristic velocity, or thrust coefficient (any one, depending upon

which two are selected as class 1 data for adjustment by the program); and RCS flow rates and axial thrust.

Class 3 data are standard spacecraft parameters used in the program. These data consist of the following items: mathematical models, tables of oxidizer and fuel volume as functions of propellant level, and miscellaneous flow-rate schedules (ablative nozzle weight loss).

## Postflight Performance Analysis

Basically, the postflight performance analysis consists of using the analytical tools and methods discussed previously to reconstruct the portion of the mission that is of interest to determine the inflight performance of the propulsion system. Comparisons of these results with predictions are made to evaluate the accuracy of the preflight prediction techniques and to determine if improvements in the prediction

techniques are required. A mission reconstruction for the purpose of a postflight analysis of the propulsion system involves the determination of the proper initial conditions at the beginning of the time segment to be analyzed, and then use of APAP to establish a best estimate (in a minimum-variance sense) of the propulsion system performance parameters.

Unlike preflight analyses, an accurate determination of APS actual flight performance from postflight analysis requires that the effects of the RCS be considered. Because the APS engine is mounted in a fixed position in the ascent stage and has no gimbal capability, the RCS is required to maintain attitude control during APS firings. Because of the changing ascent-stage center-of-gravity location during the burn as propellants are consumed and because of the thrust-vector shift during the burn that is characteristic of the ascent engine, RCS attitude control is needed throughout the burn to offset the moments caused by the APS engine thrust vector not passing through the center of gravity of the vehicle.

During the APS burn, upfiring RCS thrusters normally are inhibited to increase the  $\Delta V$  capability of the vehicle. Because of this operational mode, the RCS contributes to the thrust acceleration and to the  $\Delta V$  experienced by the ascent stage. An additional complication results from the interconnecting of the APS and RCS feed systems. During the APS burn, the interconnect valves between the two feed systems are opened, and the RCS uses APS propellant to maintain attitude control. This mode of operation ensures against the depletion of RCS propellant by a large moment unbalance in the ascent stage during the ascent burn. Because the RCS operates at a different mixture ratio than does the ascent engine, the mixture ratio of propellant from the APS tanks is not the same as the mixture ratio of the ascent engine. Thus, the effects of the RCS must be known before the APS performance can be calculated. The RCS thrust and flow rates must be used to adjust the vehicle weight and thrust acceleration before meaningful results can be obtained for APS performance.

The RCS performance is calculated by using a class characterization of the RCS performance. The bilevel measurements of the RCS thruster solenoid are used to establish the ontime for each engine. The engine ontimes are used with the RCS performance characterization to calculate consumed APS propellant (all engines) and resultant thrust (for downfiring engines only). The results of these calculations then are approximated by curve fits (as functions of time), which are used as input to APAP.

The general approach for a flight evaluation is to calculate a vehicle weight (including propellant loads) for the beginning of the segment of the APS burn used to analyze steady-state performance and, then, to allow the APAP to vary this weight and other selected performance parameters (state variables) to achieve an acceptable data match. A decision must be made to (1) believe the flight data and adjust the model so that a match can be achieved, (2) change the offending data, or (3) ignore it if one of the following conditions exists: the variations noted in the state variables necessary to achieve a good match are considered excessive, the flight data cannot be matched, or the residual curve shapes present an unrealistic trend. Ideally, the APAP would indicate the path to follow in a situation of this type, but the limited number of flight measurements available on the operational APS makes discrimination of this type of problem very difficult.

An instance in which modification of the model was necessary occurred during the analysis of the LM-3 APS flight. For this flight, it was determined that the only reasonable manner in which the model would match the flight results would be if the engine throat were to erode at a greater rate than expected.

## DISCUSSION OF RESULTS

The tools and techniques discussed previously have been employed in the course of performing preflight and postflight analyses of the APS performance for six Apollo missions to date. These missions are Apollo 5 (LM-1), Apollo 9 (LM-3), Apollo 10 (LM-4), Apollo 11 (LM-5), Apollo 12 (LM-6), and Apollo 13 (LM-7). The flights of Apollo 9, 10, and 11 are considered particularly significant from the standpoint of evaluating APS performance, and the analyses relating to these flights will be discussed in detail.

The Apollo 5 results will not be discussed, primarily because of hardware differences between LM-1 and subsequent LM vehicles. The LM-1 APS used an ascent engine with an injector built by one contractor, but all subsequent LM flight vehicles used an ascent engine with an injector built by another contractor. Because of this difference, the performance data obtained from LM-1 has less applicability to the family of LM vehicles than data obtained from subsequent flights. The Apollo 12 results are not discussed in detail because of the similarity between the Apollo 11 and 12 flights. Because the Apollo 13 mission was aborted, the LM-7 APS was not fired during the mission.

The Apollo 9 mission included the first manned flight of a lunar module, the LM-3 vehicle. The LM-3 APS was used for two firings, a 2.9-second manned firing and an unmanned burn to oxidizer depletion. The LM-3 vehicle was the last LM to carry the comprehensive developmental flight instrumentation. The LM-4 vehicle was flown during the Apollo 10 mission, which was the first flight test of the LM in the lunar environment. The LM-4 mission duty cycle consisted of two burns, a 15.6-second manned burn and an unmanned burn to fuel depletion. The Apollo 11 flight involved the performance of the design mission of the Apollo spacecraft. The LM-5 APS was used for the design mission duty cycle of a single burn to take the LM ascent stage from the lunar surface to lunar orbit. For these three flights, the results of the preflight analysis are summarized, and the performance of the APS during the mission and the post-flight analysis efforts and results are discussed.

### LM-3 Results

The LM-3 vehicle was flown in earth orbit during the Apollo 9 mission, which began on March 3, 1969. This was the first manned flight of the lunar module. The APS duty cycle consisted of a 2.9-second manned firing, which occurred at approximately 97 hours into the mission, followed 5 hours later by an unmanned firing to propellant depletion. This flight was considered particularly important from an analysis standpoint because LM-3 was the final vehicle to carry the more comprehensive developmental flight instrumentation. Although some minor anomalies were noted in the APS operation, both burns were performed successfully.

The third and final revision of the LM-3 APS preflight report was distributed in December 1968. The revisions had been necessitated by changes in the APS engine for LM-3 and by changes in the APS propellant loads. The predicted performance values, which included the estimated effects of APS propellant usage by the RCS, are shown as a part of table V. One mission objective was to terminate the second APS burn by oxidizer depletion. The preflight analysis was used to determine propellant loads, and predicted depletion of the oxidizer at 340 seconds into the second burn, leaving 33.1 kilograms (73 pounds) of usable fuel.

TABLE V. - RESULTS OF LM-3 FLIGHT ANALYSIS

Parameter	Thrust, N (lb <sub>f</sub> )	I <sub>sp</sub> , sec	Mixture ratio
Engine acceptance test <sup>a</sup>	15 609 (3509)	310.1	1.610
Predicted flight performance <sup>b</sup>	15 475 (3479)	310.1	1.606
Calculated flight performance <sup>b</sup>	15 035 (3380)	309.7	1.601
Flight performance reduced to SIC <sup>a</sup>	15 480 (3480)	310.3	1.608

<sup>a</sup>Values corrected to standard interface conditions (SIC) (117 N/cm<sup>2</sup> (170 psia) interface pressure, 294° K (70° F) propellant temperature, and acceptance test throat area).

<sup>b</sup>Average values over the mission duty cycle.

During the mission, the LM was out of range of ground tracking stations when the first APS burn was performed. When data links were reestablished after the burn, all parameters were nominal. Subsequent conversations with the crewmen confirmed that the first burn had gone as expected. During the second burn, system pressures were lower than expected, indicating a malfunction in the primary leg of the helium-regulator package. The lower system of pressures produced no harmful system effects, and the burn was terminated by oxidizer depletion at 362 seconds.

As a first step in the postflight analysis, the actual history of the regulator outlet pressure from flight was used to drive the PATS model in a reproduction of the expected vehicle performance, given the actual regulator performance. The purpose of this action was to determine how closely the preflight prediction model would reproduce the remainder of the APS flight data with the regulator performance known. This procedure gives a first-cut assessment of APS performance and should reveal significant anomalies. The reproduction was judged qualitatively to be a good representation of the flight data and, at the time of the Apollo 9 Mission Report, was the best available assessment of APS performance.

Subsequent postflight analysis with APAP indicated a basic conflict between the flight data and the engine-performance characterization. The trends noted in the system pressures could not be explained with nominal engine operation. This problem was resolved by use of the "noise in the state" option in APAP. This option allows one of the propulsion-model state variables to be adjusted during the burn in arriving at a minimum-error solution. With the use of the DFI measurement data, sufficient APS measurements were available to allow this option to be used with confidence.

Through the use of APAP "noise in the state" analysis, a higher than expected engine-throat erosion rate was found to be the only parameter that would satisfactorily explain the flight data. The engine-throat area calculated by the APAP to fit the flight data is shown and compared to the expected curve in figure 8. As seen in this figure, erosion increased the throat area by 5.3 percent at the end of the burn (based on the initial throat area) compared to the expected value. This amount of erosion exceeds (by more than a factor of 2) that seen in the ground testing of the Rocketdyne engine.

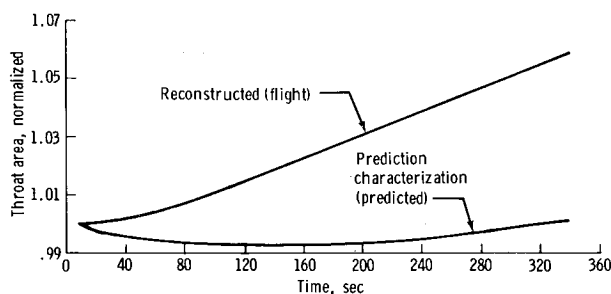


Figure 8. - LM-3 APS performance analysis results: comparison of predicted and reconstructed throat area.

An additional discrepancy noted on this flight was that the burn time was less than expected (once the lower system pressures were accounted for). In investigating this discrepancy, it was found that the mass of APS propellant that was classified as unusable because of being trapped in the zero-g can in the propellant tanks was incorrect. After this adjustment was made, the depletion was still early by approximately 3 seconds. The remainder of the discrepancy was attributed to propellant sloshing in the tanks, causing the outlet to be uncovered prematurely.

When the APAP analysis was completed, the calculated performance values were as follows: mission-duty-cycle average  $I_{sp}$ , 309.7 seconds; average mixture ratio, 1:601; and average thrust, 15 035 newtons (3380  $lb_f$ ). The APAP-calculated mixture ratio, thrust, specific impulse, and two PATS predictions are plotted as a function of time in figure 9. One of the predictions is that used in the LM-3 preflight report. Because the regulator problem resulted in operation at much lower pressure levels, a second prediction was made using flight data of the regulator outlet pressure discussed earlier.

The more extensive instrumentation of the LM-3 vehicle made possible a more comprehensive flight-performance evaluation than has been accomplished on subsequent missions. The feedline  $\Delta P$  transducers were of particular importance in establishing propellant flow rates and mixture ratio. The manner in which engine-throat erosion affects the  $\Delta P$  and chamber-pressure measurements is shown in figure 10 as a comparison of the PATS reprediction (using flight-regulator data), the APAP reconstruction, and the actual flight measurements.

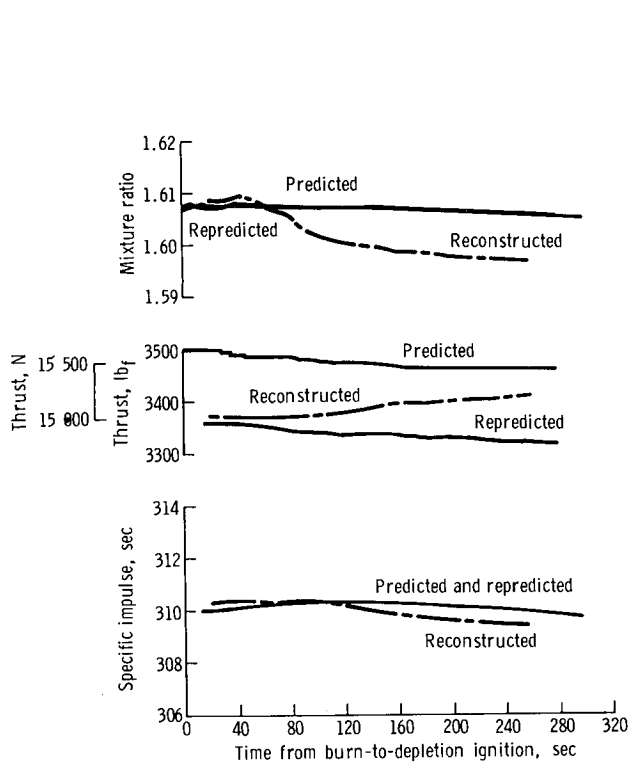


Figure 9. - LM-3 APS performance analysis results: comparison of predicted and reconstructed performance.

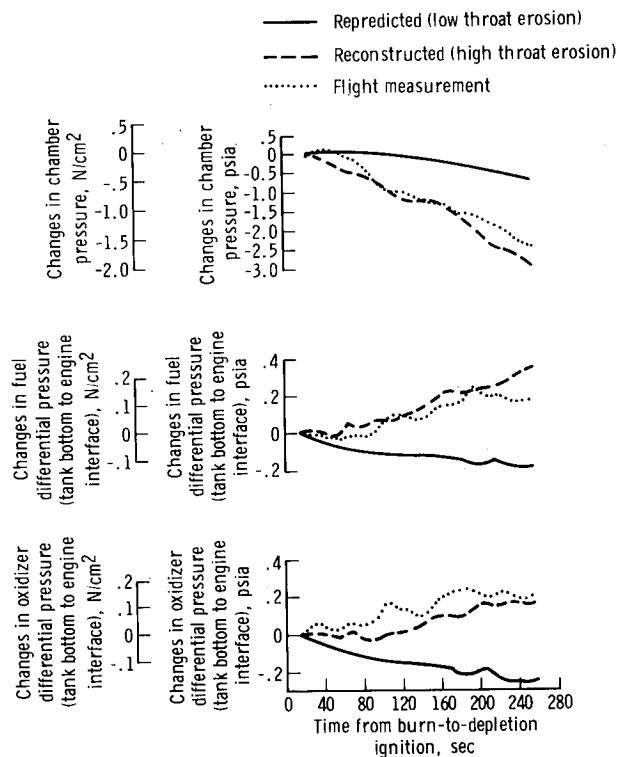


Figure 10. - LM-3 APS postflight performance analysis: comparison of pressure trends (flight, reconstructed, and repredicted).

A comparison of actual to preflight-predicted temperature and pressure histories of the helium-storage tanks is presented in figures 11 and 12. A comparison of actual to predicted regulator outlet pressure is illustrated in figure 13. The quality of the flight reconstruction is depicted in figures 14 to 19. The primary measurements used in the APAP analysis and their residuals (the difference between the actual measurement and the value calculated by the program for that measurement) are shown. The measured flight data given in these figures are not the raw data but are the data after editing and filtering operations have been performed to make them more palatable to the APAP. A quantitative measure of the quality of the reconstruction is provided by the slope, intercept, and variance values given in figures 12 to 17. These data represent the intercept (at the ordinate) and the slope of a first-order curve fitted to the residual plot. The variance is a measure of how well the residual data are represented by the straight line. The nearer the slope and intercept approach zero, the better the match between the flight data and the reconstruction. Plots of oxidizer and fuel interface pressure have zero residual because the APAP uses these two measurements to drive the simulation and to match the remainder of the data (figs. 14 and 15).

The best-fit solution concluded that small negative biases (in which the model considers the flight data to be reading erroneously low) exist on the feedline  $\Delta P$  measurements and that the chamber-pressure-transducer output has a positive drift during the burn (figs. 16 to 18). The good match of vehicle acceleration obtained is illustrated in figure 19.



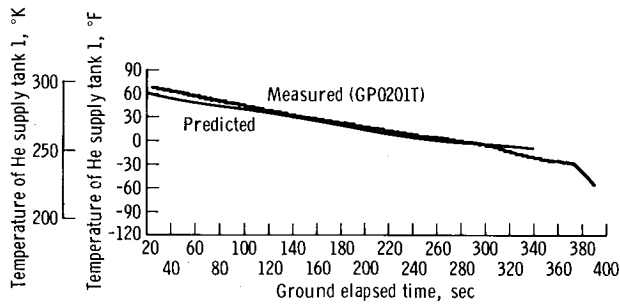


Figure 11. - LM-3 APS flight results: predicted and actual helium source temperature.

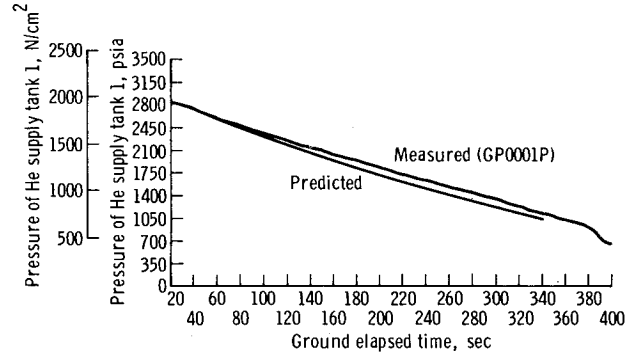


Figure 12. - LM-3 APS flight results: predicted and actual helium source pressure.

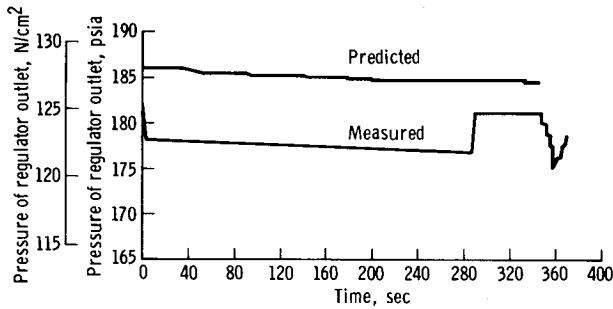


Figure 13. - LM-3 APS flight results: predicted and actual helium-regulator outlet pressure.

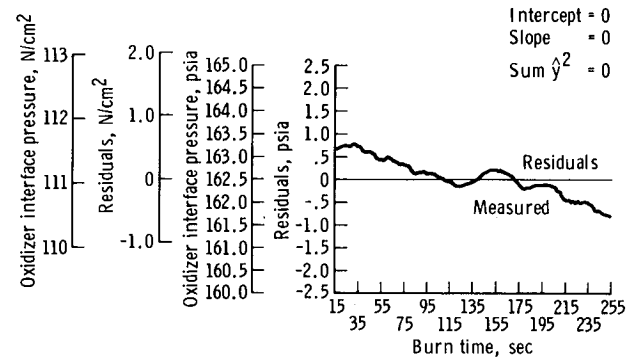


Figure 14. - LM-3 APS flight results: oxidizer interface pressure.

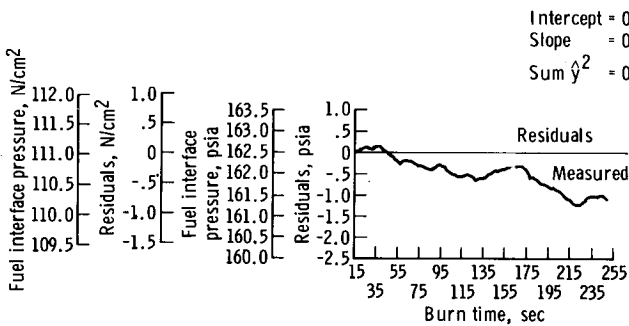


Figure 15. - LM-3 APS flight results: fuel interface pressure.

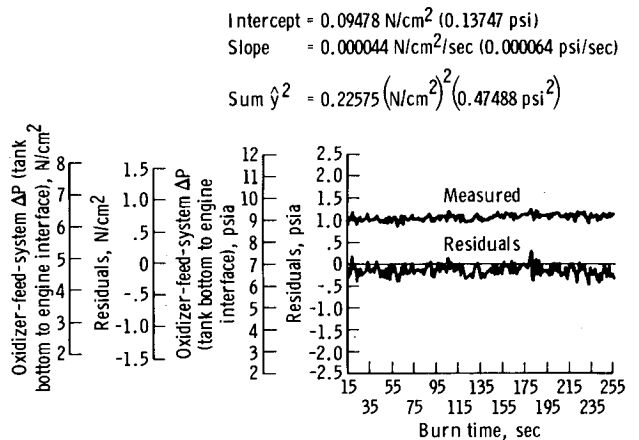


Figure 16. - LM-3 APS postflight performance analysis: oxidizer-feed-system differential pressure (tank bottom to engine interface).

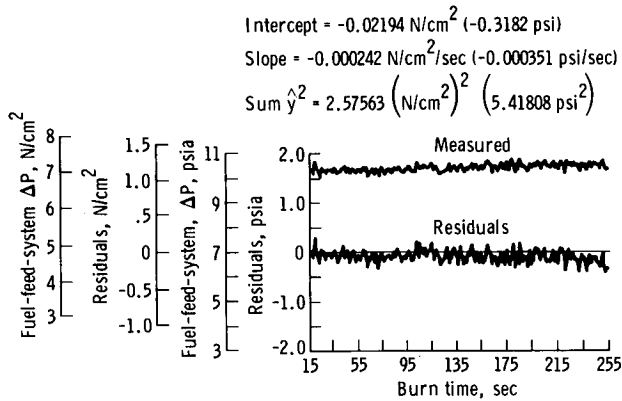


Figure 17. - LM-3 APS postflight performance analysis: fuel-feed-system differential pressure (tank bottom to engine interface).

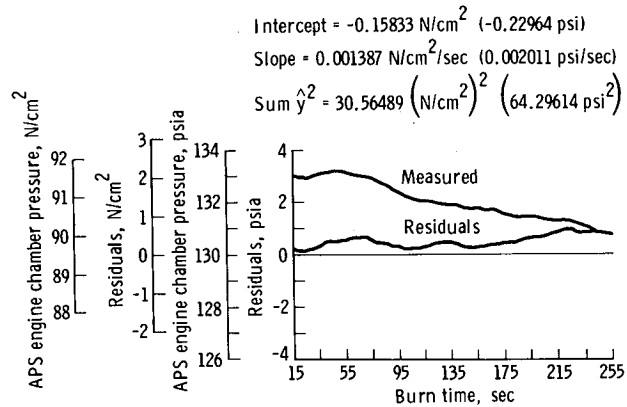


Figure 18. - LM-3 APS postflight performance analysis: engine chamber pressure.

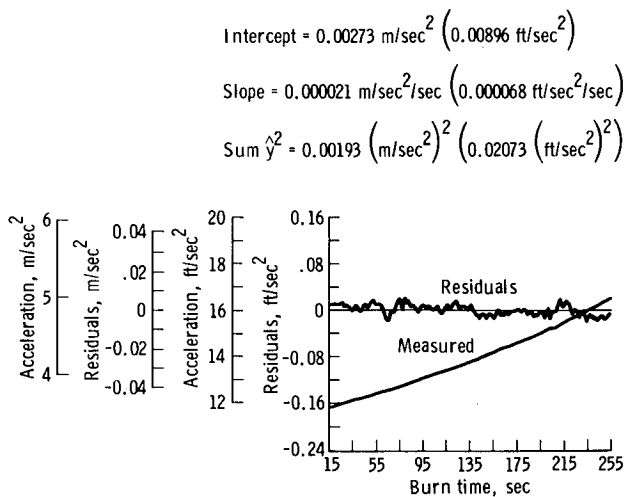


Figure 19. - LM-3 APS postflight performance analysis: ascent-stage thrust acceleration.

The performance parameters associated with the LM-3 engine are listed in table V. The first set of values contains the averaged results of four altitude acceptance tests performed at the facility of the contractor. The values have been corrected to standard interface conditions. The second set of values, which contains the predicted flight results obtained from a PATS simulation, consists of the average values over the simulated mission duty cycle. These values are not at standard interface conditions; they are at the interface conditions predicted to occur by the APS model. The third set of values consists of the performance parameters calculated from flight data. Again, these values are at the actual interface conditions occurring in flight. The final set of values results from correcting the calculated flight performance to standard interface conditions. In this case, standard interface conditions also include

the preflight engine-throat area. A comparison of the first and last sets of values indicates the repeatability of the engine performance. A comparison of the second and third sets of data illustrates the validity of the preflight prediction.

A more detailed discussion of the LM-3 postflight analysis results and a complete listing of the flight data obtained during the APS firings can be found in reference 5.

## LM-4 Results

The LM-4 vehicle was flown during the Apollo 10 mission, which was launched on May 18, 1969. This mission was the second manned LM flight and the first flight test of the LM in the lunar environment. The APS duty cycle consisted of two firings, a manned firing of 15.6-second duration that occurred at approximately 103 hours into the mission and an unmanned burn to propellant depletion 6 hours later. A test objective of this flight was to confirm that a propellant-depletion shutdown in space is not hazardous.

The LM-4 APS preflight performance analysis was incorporated into the LM SODB in March 1969 and was revised in May to reflect changes in propellant loading. The APS propellant load was reduced to approximately 50 percent of the capacity, and the remainder was biased to ensure a fuel-first propellant depletion. The effect of the RCS on APS parameters was not included in the LM-4 analysis. The predicted performance values are shown as a part of table VI. The preflight analysis neglecting the effect of the RCS, predicted that the second APS burn would be terminated by fuel depletion after 215 seconds.

TABLE VI. - RESULTS OF LM-4 FLIGHT ANALYSIS

Parameter	Thrust, N (lb <sub>f</sub> )	I <sub>sp</sub> , sec	Mixture ratio
Engine acceptance test <sup>a</sup>	15 578 (3502)	308.6	1.612
Predicted flight performance <sup>b</sup>	15 480 (3480)	308.4	1.589
Calculated flight performance <sup>b</sup>	15 266 (3432)	309.5	1.597
Flight performance reduced to SIC <sup>a</sup>	15 627 (3513)	309.3	1.594

<sup>a</sup>Values corrected to standard interface conditions (SIC) (117 N/cm<sup>2</sup> (170 psia) interface pressure, 294° K (70° F) propellant temperature, and acceptance test throat area).

<sup>b</sup>Average values over the mission duty cycle.

Several exceptions to expected performance were noted during the mission. These exceptions were as follows: the oxidizer-interface-pressure transducer (GP1503P) experienced a postlaunch shift, the APS warning light indicating low propellant level came on during the first APS burn, the helium-regulator outlet pressure was lower than expected during both burns, and oscillations were noted in the output

of the helium-regulator outlet-pressure transducers. None of these problems interfered with the operation of the APS or with the successful accomplishment of the mission.

As was done for the LM-3 analysis, the first step in the postflight analysis was performance of an after-the-fact simulation of the APS mission duty cycle, using PATS with actual flight data used for helium-regulator outlet pressure and propellant temperatures. This simulation compared closely with flight results, reaffirming nominal system operation. The postflight PATS simulation indicated that the fuel-tank low-level sensor should have been uncovered at 200 seconds into the second burn. The actual time for this event was 199 seconds. The chamber pressure began to decay at 207 seconds (indicating fuel depletion), and the oxidizer low-level sensor was uncovered at 212 seconds. The engine was commanded off 248 seconds after ignition.

Analysis efforts with APAP verified that the oxidizer-interface-pressure transducer was biased by  $7.58 \text{ N/cm}^2$  (11 psi) (high) as reported in the mission report and that the fuel-interface-pressure transducer had a positive  $1.38 \text{ N/cm}^2$  (2 psi) bias. Because the RCS/APS interconnect was not opened during the mission, calculation of the APS mixture ratio was considerably simplified. With the low-level-sensor actuation times, in addition to the normally available flight data, calculations revealed that the average mixture ratio was 1.597. A comparison of acceptance test results, predicted performance, and calculated performance is presented in table VI. The predicted performance values as a function of time during the burn, as compared with the actual values, are depicted in figure 20. In contrast to the LM-3 results, the APAP analysis revealed that the engine-throat erosion was approximately as expected.

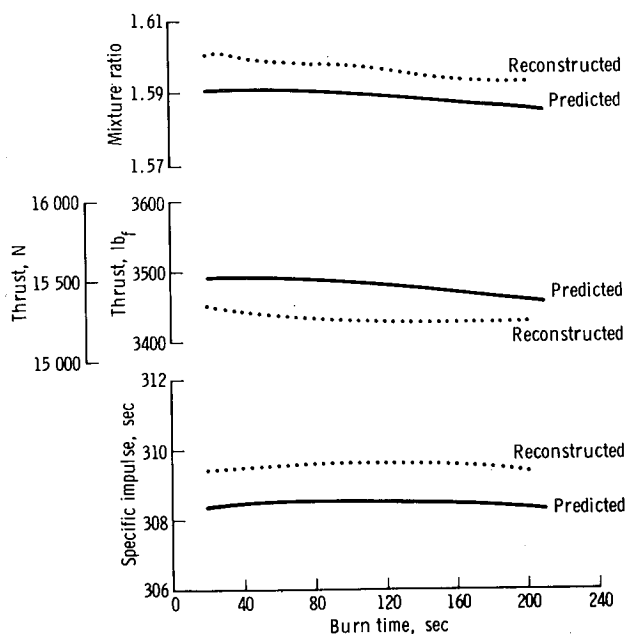


Figure 20. - LM-4 APS performance analysis results: comparison of predicted and flight-reconstructed performance.

The detailed results of the postflight analysis efforts on the LM-4 APS are presented in reference 6. This reference also contains a complete listing of the APS flight data.

## LM-5 Results

The LM-5 vehicle was flown during the Apollo 11 mission, launched on July 16, 1969. This was the third manned flight of the lunar module and the first manned lunar-landing mission. The APS duty cycle consisted of a single burn of 435 seconds (from the lunar surface to an 89- by 17-kilometer (48- by 9-nautical-mile) lunar orbit). All aspects of APS operation were nominal throughout the ascent.

The LM-5 preflight report, incorporated into the LM SODB in March 1969, was updated in May. The values presented in the second SODB amendment were the same

as those given in the LM-5 APS preflight report (ref. 7), which was published in June 1969. Because the decision was made earlier to neglect RCS interaction in determining APS preflight performance, the duty cycle used for the preflight simulations was a single burn to propellant depletion from a full propellant load. By simulating a burn to depletion, the mission planner was afforded flexibility in areas of ascent-stage lift-off weight, cut-off velocity in lunar orbit, and RCS propellant requirements from the APS, all of which affect the actual burn time of the APS required for orbital insertion.

Two events reduced the confidence in the preflight predictions for LM-5. The LM-5 was the first vehicle to be fitted with a C-series Rocketdyne ascent engine. The C-series engine incorporated a thrust chamber and nozzle of the same contour as earlier engines but was constructed of a different (lightweight) material. Because the performance characterization was based on test data from engines fired with the heavy-weight chamber, the applicability of the characterization for predicting specific-impulse variation with burn time and throat-erosion rate was in doubt, but the limited testing performed with the lightweight chamber at the time seemed to confirm that the characterization was adequate. The second problem was that the engine propellant filters were changed after the engine had been through acceptance testing. Data obtained from flow testing of the new filters before the installation were used to adjust the acceptance test data for the actual engine (flight configuration) resistances.

The only exception to expected system operation occurred following the ascent burn. Shortly after ascent, the ascent stage went behind the moon, and no data were available for approximately 50 minutes. At reacquisition of signal, drops of 4.1 and 2.5 N/cm<sup>2</sup> (6 and 3.6 psi) had occurred in the oxidizer- and fuel-interface-pressure measurements. The APS data were received for 4.5 hours, and the pressures held constant during that time. This event is discussed thoroughly in reference 8. No single mechanism that would explain the observed data has been identified; however, leakage is not considered a cause because the pressures were constant for 4.5 hours following the indication of the pressure decrease, and the apparent pressure drop had no effect on APS performance.

The postflight reconstruction was complicated by the lack of measurements indicating APS propellant quantities or flow rates. The propellant feedline  $\Delta P$  transducers, which gave an accurate indication of propellant flow rate and mixture ratio, were removed from vehicles following the LM-3. The propellant-tank low-level sensors, although active measurements for LM-5 (and subsequent vehicles), were not uncovered during the burn as on LM-3 and LM-4. This lack of flight instrumentation necessitates that the propellant and feedline resistances be assumed unchanged from the values determined in preflight testing. Although this assumption was made during analysis of earlier flights as a first approximation, other data were available to evaluate the validity of that assumption. Because the engine performance is a very weak function of mixture ratio over the range of interest, no means existed for verifying fluid-flow resistances in flight.

Accurate simulation of RCS activity was especially important in the LM-5 analysis because the RCS thrusters were not fired in a coupled mode during the ascent and, therefore, provided a net contribution to the  $\Delta V$  obtained by the ascent stage. In addition, the RCS used APS propellant through the APS/RCS interconnect during the ascent

burn. To accurately assess APS performance, these effects must be known so that APS and RCS effects can be separated. The RCS ontimes obtained from the thruster-solenoid bilevel measurements were multiplied by nominal values of RCS thrust and flow rates to obtain the desired values as functions of time (fig. 21).

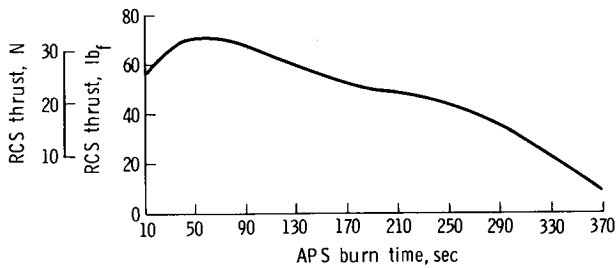


Figure 21. - LM-5 APS postflight performance analysis: time-averaged RCS thrust.

The performance values obtained from the APAP analysis, the results obtained from acceptance testing of the LM-5 engine, the preflight-predicted performance, and the flight results corrected to standard interface conditions are presented in table VII. Because of the limited number of APS flight measurements available, determination of a mixture-ratio shift is difficult, and determination of whether the shift is caused by feed system or engine problems is not possible. Thus, reduction of engine performance to standard interface conditions will give the engine mixture ratio from acceptance testing and could mask actual engine problems.

Predicted and reconstructed performance parameters for the LM-5 mission are compared in figure 22. Although some doubt had been expressed earlier regarding the ability of the engine model to predict throat-erosion rates for the modified (lightweight) chamber, the throat area as compared to the time curve calculated during the flight reconstruction agreed closely with the preflight prediction.

TABLE VII. - RESULTS OF LM-5 FLIGHT ANALYSIS

Parameter	Thrust, N (lb <sub>f</sub> )	I <sub>sp</sub> , sec	Mixture ratio
Engine acceptance test <sup>a</sup>	15 511 (3487)	309.7	1.605
Predicted flight performance <sup>b</sup>	15 320 (3444)	309.3	1.598
Calculated flight performance <sup>b</sup>	15 311 (3442)	310.8	1.606
Flight performance reduced to SIC <sup>a</sup>	15 551 (3496)	310.8	1.596

<sup>a</sup>Values corrected to standard interface conditions (SIC) (117 N/cm<sup>2</sup> (170 psia) interface pressure, 294° K (70° F) propellant temperature, and acceptance test throat area).

<sup>b</sup>Average values over the mission duty cycle.

## General Comments

The results of performance analysis efforts as applied to the three APS missions discussed previously have demonstrated the capability that exists for prediction and measurement of propulsion system performance. In general, the agreement between predicted and calculated performance values is quite good. The difference between predicted and calculated performance exceeds the preflight prediction uncertainty band in only one case, that being the predicted thrust for LM-3, in which a hardware malfunction was experienced.

Continuing problems for the APS analysis efforts are primarily associated with the small number of flight-data measurements available on the operational vehicles. The lesser number of flight measurements increases the difficulty of establishing flight performance from several aspects: inflight transducer shifts and biases are more difficult to establish with fewer measurements to compare; the erosion characteristics of the ablative engine throat are more difficult to separate from other effects; and the actual engine mixture ratio is difficult to determine.

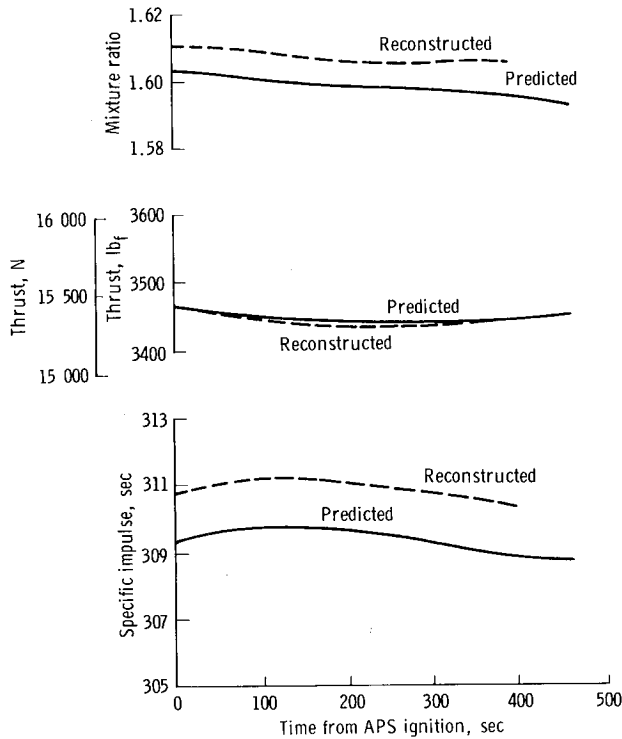


Figure 22. - LM-5 APS performance analysis results: comparison of predicted and reconstructed performance.

Because the engine-performance parameters are a weak function of mixture ratio (over the range of concern) and because the APS has no propellant gaging system (with the exception of the propellant-tank low-level sensors, which are not uncovered in a nominal mission duty cycle), sufficient information was not available from the APS operational instrumentation to allow a meaningful calculation of mixture ratio. This problem was overcome by the adoption of a method that involves calculation of the center of gravity of the ascent stage as a function of time during the APS burn. The ascent-stage center of gravity is calculated from the amount of RCS activity necessary to maintain the vehicle attitude. The mixture ratio of the propellant consumed is then related to the calculated center-of-gravity travel.

An error analysis of this method revealed that the uncertainty associated with the center-of-gravity-calculated mixture ratio, although greater than the uncertainty band associated with the preflight prediction of mixture ratio, was acceptable and represented a significant improvement over the previously used method of assuming constant resistances.

## CONCLUDING REMARKS

The flight results obtained to date have demonstrated that the tools and techniques developed by the Manned Spacecraft Center for performance analysis of the ascent propulsion system are capable of predicting the performance expected from the ascent propulsion system within the quoted accuracy bands for the nominal system performance and for selected off-nominal conditions. The efforts expended by the Manned Spacecraft Center and the various contractors in performing the propulsion system analyses for the Apollo vehicles have resulted in several benefits and have satisfied the primary goal of predicting the propulsion system performance and establishing realistic uncertainty bands associated with the prediction. These benefits include the following.

1. Advances have been made in mathematical techniques in developing the computer program used for postflight performance analysis. This statement refers to the creation of algorithms that allow the postflight analysis computer program to calculate the partial derivatives required for the minimum-variance estimation from the user-supplied system model.

2. Advances have been made in data processing techniques for handling large amounts of high-sample-rate data obtained from flight and ground tests. These advances are concerned with the operations conducted on propulsion system telemetry data. The operations involved in the processing of flight data are considered unique because of the speed and efficiency of the computer programs used to perform these operations.

3. An enhancement of system-malfunction detection and analysis capability is evident. The propulsion system models, developed for use in preflight and postflight performance analysis, were constructed with sufficient generality to also allow the study of off-nominal and malfunction operation. By this capability, the various malfunctions can be simulated, and their effect on the propulsion system can be assessed.

4. The potential for reducing ground test requirements is apparent. With a sufficiently general model that is based on the propulsion system physical characteristics, studies can be made of the response of the propulsion system to changes in various parameters to define the system operation over a wide band of conditions. The results of these studies can be used to set up ground test programs for the propulsion system.

Lyndon B. Johnson Space Center  
National Aeronautics and Space Administration  
Houston, Texas, September 28, 1973  
914-50-60-07-72



## REFERENCES

1. Baumgartner, A. T.: User's Manual for PATS, Propulsion Analysis Trajectory Simulation Program. NASA CR-134025, 1968.
2. Seto, R. K. M.: Propulsion Systems Dispersion Analysis and Optimum Propellant Management. NASA CR-92458, 1968.
3. Powers, C. S.; and Smith, L. H.: Oracle-Mafia Program, Volume I. NASA CR-134015, 1967.
4. Landry, D. G.: Model Compiler—A Symbolic Input Processor Interfaced With the Propulsion Analysis Program, Volume I. NASA CR-134017, 1969.
5. Thompson, P. F.; and Griffin, W. G.: Apollo 9 LM-3 Ascent Propulsion System, Final Flight Evaluation. NASA CR-109943, 1969.
6. Griffin, W. G.: Apollo 10 LM-4 Ascent Propulsion System Final Flight Evaluation. NASA CR-109930, 1969.
7. Thompson, P. F.; and Johnston, C. G.: Apollo Mission G/LM-5APS Preflight Performance Report. NASA CR-134024, 1969.
8. Thompson, P. F.: Apollo 11 LM-5 Ascent Propulsion System Final Flight Evaluation. NASA CR-102151, 1969.

## APPENDIX

### ABBREVIATIONS AND ACRONYMS

APAP	Apollo Propulsion Analysis Program
APS	Ascent Propulsion System
C*	Characteristic Exhaust Velocity
DFI	Developmental Flight Instrumentation
GAC	Grumman Aerospace Corporation
ISP	Specific Impulse
JSC	Lyndon B. Johnson Space Center
LGC	LM Guidance Computer
LM	Lunar Module
MC	Model Compiler
MSC	Manned Spacecraft Center
MVE	Minimum-Variance Estimation
PATS	Propulsion Analysis Trajectory Simulation Program
PCM	Pulse-Code Modulation (operational instrumentation)
PIT	Pre-Installation Testing
RCS	Reaction Control System
SODB	Spacecraft Operational Data Book
WSTF	White Sands Test Facility